# WHITE PAPER

## ENERGY BUFFERS

**John Miller, JNJ Miller, P.L.C., Cedar, MI**
**Patrick J. McCleer, McCleer Power, Inc., Jackson, MI**
**Mark Cohen, Maxwell Technologies, Inc. ®, San Diego, CA**

## 1. Introduction

Today ultracapacitors are proving to be useful as high power energy accumulators in hybrid electric power trains. The Nissan supercapacitor truck for example uses a 384 cell module consisting of three, 128 cell strings of 1500 F, 2.7V cells in parallel and delivers 583 Wh. The Nissan supercapacitor truck, Condor, is powered by a 7.0 liter CIDI engine rated at 152 kW in a parallel hybrid architecture with a 55 kW permanent magnet motor. The Condor supercapacitor bank is capable of an impressive 6.3 Wh/kg and has a P/E of 80 [1]. Honda Motor Co. has applied ultracapacitors as high power buffers to the fuel cell stack used in their FCX line of hybrid vehicles commencing with the FCXV3 in 2000. Honda maintains the use of ultracapacitors in the FCX line including the V4 introduced in 2001, and on through the most recent introduction of FCX in 2003 [2]. Toyota Motor Co. has developed an experimental vehicle to showcase their clean diesel technology. The Toyota ES 3 achieved a fuel consumption of 2.13 liter/100 km on the Japan 1015 mode [3]. The ES 3 propulsion system is derived from its sister vehicle, the European Yaris, that employs a 1.4 liter, I4, TDI engine. Equipped with common rail injection, variable ratio turbo, and a compact CVT the ES 3 is seen as a pioneering vehicle in low fuel consumption clean diesel technology. The key to low fuel consumption is the energy regenerator hybrid technology depicted in Figure 1. The ES 3 power train is conventional in all respects except for the electric M/G integrated into the CVT in a post-transmission parallel hybrid architecture. No specifics are given for the ultracapacitor rating other than it is high voltage.

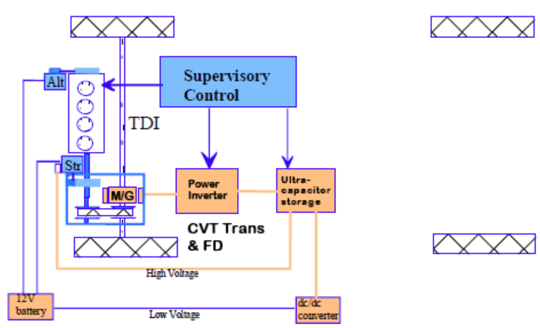


*Fig. 1 ES[3] clean diesel ultra-capacitor hybrid*

Low fuel consumption is achieved through idlestop power train control and in part from a regenerative brake system that is augmented by a high voltage ultracapacitor energy storage module. Vehicle braking energy is recuperated by the M/G regenerator and fed to the energy storage module. From there the recovered energy is used in part for warm restart of the engine and in part to sustain vehicle loads on the low voltage power network. A dc/dc converter is used to regulate the variable voltage from the ultracapacitor to the vehicles 12V battery. An engine driven alternator replenishes the storage battery when the engine is running. In addition to the hybrid functionality the vehicles brake system also maintains grade holding during engine off periods. Cabin climate control is sustained during idle stop by a cooling storage device so that air conditioning is available at all times. Other investigators continue to explore the application of ultracapacitors to hybrid power trains. The Paul Scherrer Institute (PSI, Switzerland) in collaboration with the Swiss Federal Institute of Technology (ETHZ) have equipped a 48 kW fuel cell vehicle with a 360 Wh ultracapacitor bank sized for peak power [4]. In this architecture the ultracapacitor assists the fuel cell power plant during periods of high pulse power loading such as vehicle launch and deceleration in order to optimize vehicle efficiency. The PSIETHZ hybrid vehicle propulsion system architecture is similar to that shown in Figure 2.

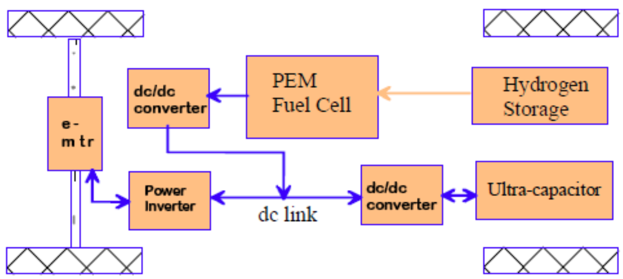


*Fig. 2 Hy-Power ultra-capacitor hybrid (PSI-EHTW)*

The ultracapacitor energy storage unit illustrated in Figure 2 provides all transient power for the vehicles propulsion system during launch and braking. Rated at 50 kW pulse power for 15s the ultracapacitor sustains vehicle drive line power demands during the fuel cell transient interval (nominal 2.5 kW/s but limited to 1 kW/s in the HyPower vehicle tests). The traction motor is rated 45 kW continuous and 75 kW peak off the 360 V dc link. The operational strategy in the case of the HyPower architecture was to base load the fuel cell and rely on the ultracapacitor bank for transient performance. Test weight of the VW Bora experimental vehicle was held at 2000 kg during NEDC fuel consumption testing. Fuel consumption over the NEDC cycle amounted to less than 7 liter/100 km. For comparison the fuel consumption of a similar weight class, but non-hybridized, vehicle such as the BMW 7 series is 10.7 liter/100 km. During a launch transient the ultracapacitor energy cache discharges at its limit of pulse power then decays linearly as the fuel cell power plant power ramps to a steady state value.

Fuel cell vehicle architectures having the fuel cell stack interfaced to the dc link via a dc/dc booster are receiving much attention as the system described in Figure 2 has shown. Hyundai Motor Co. is also investigating fuel cell power plants with dc/dc booster but with a battery in place of the ultracapacitor in Figure 2 [5]. The logical extension to the vehicle propulsion architectures given in [4] and [5] has been developed in the form of a multiple-input dc/dc converter as interface to the traction battery pack, the electric peaking power ultracapacitor energy storage, and to an engine driven generator by the investigators at the University of Rome [6]. Figure 3 is representative of the multiple-input converter hybrid drive train.

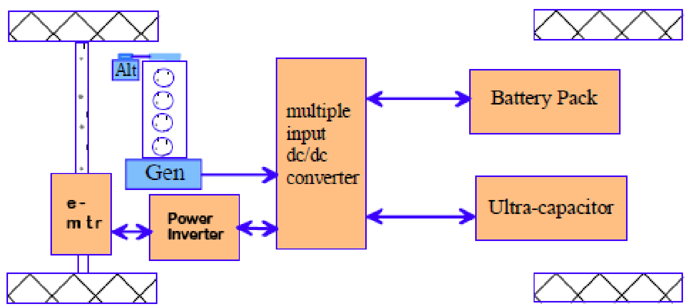


*Fig. 3 Multiple-input dc/dc converter hybrid drive train*

The system described by Figure 3 is rated 60 kW of traction power at 300 V that is supplied by an algorithm supervised combination of a 15 kW engine driven generator, a 24 Ah, 240V battery, and a 89 Wh, 240V ultracapacitor. The battery is capable of 120 A discharge and the ultracapacitor of 250 A discharge. The multiple-input dc/dc converter consists of individual buck-boost stages per energy source rated for 200 A at the common dc link to the traction motor power inverter. The propulsion power flow control algorithm seeks to maintain a balance between SOC of the battery and ultracapacitor while minimizing the fuel consumption of the engine during normal driving. In addition to power flows, the control law schedules power from each energy source according to its time response capability. The engine driven generator represents the slow branch, the battery pack the medium response branch, and the ultracapacitor the fast response branch.

Ultracapacitors have already found application in the propulsion system of conventional gasoline and diesel hybrid as well as fuel cell hybrid vehicles. The reason for the acceptance of ultracapacitors in vehicle propulsion systems is their high pulse power capability, fast transient response, and high efficiency during discharge and recharging plus full charge cycling in excess of 100k cycles. The ultracapacitor is now proven to be an able augmentation to hybrid power trains as an electrical peaking unit. In this paper the application of ultracapacitors as distributed energy storage buffers in the vehicles electrical system is investigated.

A multiple zone electrical distribution system architecture augmented with local energy buffers is one method of addressing the need for redundancy that safety critical and security systems require. New introductions of x-by-wire functionality, idle-stop power trains, and electrified engine functions such as electromechanical engine valve actuation also benefit from modular and distributed local energy buffering offered by ultracapacitors. Ultracapacitors are nonFaradic surface effect storage devices that offer pulse power and power cycling capability far in excess of Faradic, bulk storage, electrochemical cells. Power management for safety critical systems such as steer, brake and drive by wire benefit from distributed energy modules that are positioned locally, are lower in mass, and are more energetic than batteries. The combination of ultracapacitors with electrochemical batteries has already been done for traction applications, generally through a dc/dc converter interface.

## 2. Ultracapacitor Model

The ultracapacitor cell model currently under investigation by researchers at MIT [7] will form the basis for modeling the distributed energy storage module concepts in this paper. Phenomenological behavior of the highly distributed RC network that is an ultracapacitor is modeled using the three time constant equivalent circuit shown in Figure 4. The basic cell model used by the MIT research team captures the short term behavior of commercially available cells.

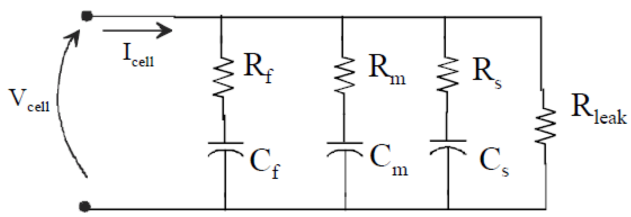


*Fig. 4 Ultra-capacitor short term equivalent circuit*

The short term equivalent circuit for an ultracapacitor cell is found to have the parameter values listed in Table 1 for a commercially available component.

| Fast branch | | Medium branch | | Slow branch | | Leakage | |
|---|---|---|---|---|---|---|---|
| $R_f$ | 0.68 mΩ | $R_m$ | 0.8 Ω | $R_s$ | 2.9 Ω | $R_{lk}$ | 3 kΩ |
| $C_f$ | 2600 F | $C_m$ | 250 F | $C_s$ | 560 F | | |
| $\tau_f$ | 1.768 s | $\tau_m$ | 200 s | $\tau_s$ | 1624 s | | |

***Table 1. Ultra-capacitor cell equivalent circuit parameters*** (courtesy MIT for 2500 F, 0.68 mΩ EDLC)

Application of the short term cell model to an N-cell module results in a complex circuit for simulation consisting of a string of the equivalent circuits shown in Figure 4. The equivalent model for an Ncell module is shown as Figure 5 for reference. In this configuration the time constants of the three branches of the short term model are retained but the simulation must solve for N(M1)+ 1 nodes instead of just M nodes per equivalent circuit.

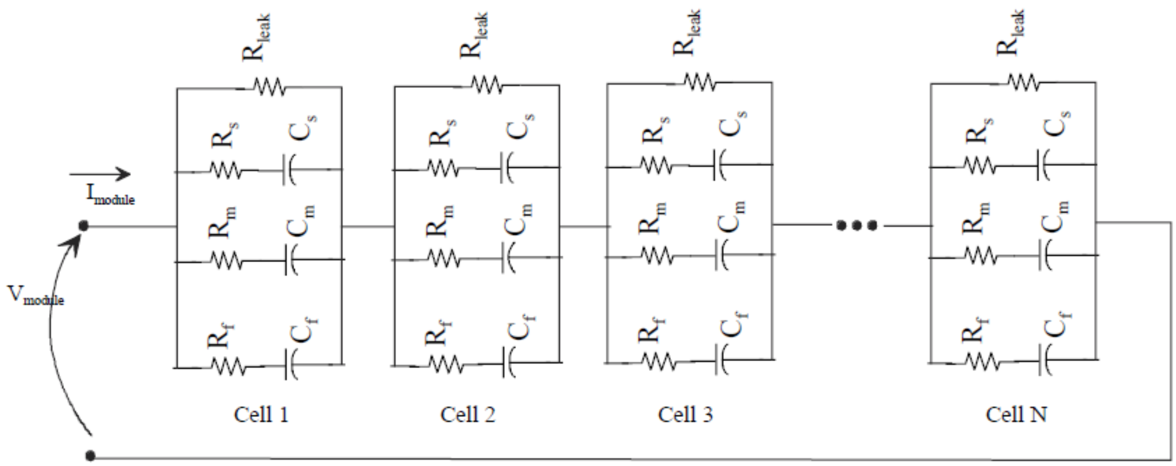


**Fig. 5 N-cell module equivalent circuit**

For an N=6 cell string used for a 14V automotive application energy buffer the module equivalent circuit given by Figure 5 is tractable, but requires knowledge of the cell parameters. Derivation of the cell parameters based on laboratory testing takes several weeks of data acquisition and reduction. It would be far more convenient to use data sheet cell parameters and scale to arbitrary cell count modules in order to more readily apply ultracapacitors to vehicle electrical distribution system applications as distributed modules. In order to accomplish this we chose to scale according to the rules listed in Table 2 that retain the basic short term model branch time constants.

**Maxwell Technologies, Inc.**
**Worldwide Headquarters**
9244 Balboa Avenue
San Diego, CA 92123
USA
Phone: +1 858 503 3300
Fax: +1 858 503 3301

**Maxwell Technologies SA**
CH-1728 Rossens
Switzerland
Phone: +41 (0)26 411 85 00
Fax: +41 (0)26 411 85 05

**Maxwell Technologies GmbH**
Brucker Strasse 21
D-82205 Gilching
Germany
Phone: +49 (0)8105 24 16 10
Fax: +49 (0)8105 24 16 19

**Maxwell Technologies, Inc. -**
**Shanghai Representative Office**
Rm.2104, Suncome Liauw's Plaza
738 Shang Cheng Road
Pudong New Area
Shanghai 200120, P.R. China
Phone: +86 21 5836 5733
Fax: +86 21 5836 5620

**info@maxwell.com – www.maxwell.com**

$$\phi = 0.5(\sqrt{5} - 1)$$
$$j = 2$$
$$k = 8$$

| Fast | | Medium | | Slow | | Leakage | |
|---|---|---|---|---|---|---|---|
| $R_f$ | $\frac{2}{3}ESR$ | $R_m$ | $\frac{2}{3}\phi^{-(2k-1)}ESR$ | $R_s$ | $\frac{2}{3}\phi^{-(2k+1)}ESR$ | $R_{lk}$ | $\frac{V_r}{I_{leak}}$ |
| $C_f$ | $1.05C_0$ | $C_m$ | $1.05\phi^{+(2j+1)}C_0$ | $C_s$ | $1.05\phi^{+(2j-1)}C_0$ | | |
| $\tau_f$ | $\frac{2.1}{3}C_0ESR$ | $\tau_m$ | $\frac{2.1}{3}\phi^{+2(1+j-k)}C_0ESR$ | $\tau_s$ | $\frac{2.1}{3}\phi^{+2(1+j-k)}C_0ESR$ | | |

*Table 2. Ultra-capacitor scaling model*

The model parameters listed in Table 2 may be readily scaled to an arbitrary N-cell module for an ultracapacitor having data sheet values for nominal capacitance, C0, equivalent series resistance, ESR, and leakage current $I_{leak}$ (at 72 h, 25°C, $V_r$ Volts). The short term ultracapacitor model scaled to an N-cell string (j=2 and k=8) becomes:

| Fast | | Medium | | Slow | | Leakage | |
|---|---|---|---|---|---|---|---|
| $R_f$ | $\frac{2N}{3}ESR$ | $R_m$ | $\frac{2N}{3}\phi^{-(2k-1)}ESR$ | $R_s$ | $\frac{2N}{3}\phi^{-(2k+1)}ESR$ | $R_{lk}$ | $\frac{NV_r}{I_{leak}}$ |
| $C_f$ | $\frac{1.05}{N}C_0$ | $C_m$ | $\frac{1.05}{N}\phi^{+(2j+1)}C_0$ | $C_s$ | $\frac{1.05}{N}\phi^{+(2j-1)}C_0$ | | |
| $\tau_f$ | $\frac{2.1}{3}C_0ESR$ | $\tau_m$ | $\frac{2.1}{3}\phi^{+2(1+j-k)}C_0ESR$ | $\tau_s$ | $\frac{2.1}{3}\phi^{+2(1+j-k)}C_0ESR$ | | |

*Table 3. Scaled N-cell ultra-capacitor module*

From which the module equivalent circuit for short term ultracapacitor behavioral modeling can be sketched as shown in Figure 6 below.

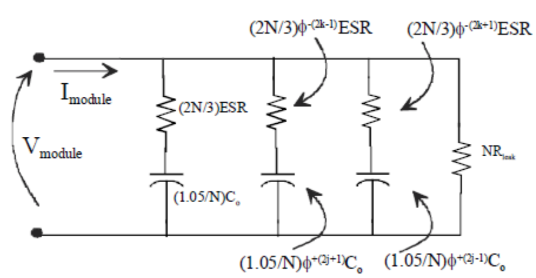


***Fig. 6 Scaled equivalent circuit of an arbitrary ultra-capacitor***

The terminal behavior of an N-cell ultracapacitor according to the short term model is given as the solution for module current in Figure 5. Likewise, the solution of its scaled equivalent is given as the module current for the circuit in Figure 6. A PSPICE simulation of the circuit in Figure 5 is performed for two cases to illustrate both time domain and frequency domain behavior. In the time domain the pulse current response is sought and in the frequency domain its frequency response function, FRF, is sought. Assuming the same 2500 F, 2.5V, 1 mΩ ultracapacitor as modeled in Table 1 we arrive at the scaled parameters for the equivalent of a 6cell string as listed in Table 4 below. The values in Table 4 are then entered into a companion PSPICE simulation to compare the performance of the scaled model of Figure 6 to the replicated model shown in Figure 5.

| Fast branch | | Medium branch | | Slow branch | | Leakage | |
|---|---|---|---|---|---|---|---|
| $R_f$ | 4 mΩ | $R_m$ | 5.45 Ω | $R_s$ | 14.28 Ω | $R_{lk}$ | 18 kΩ |
| $C_f$ | 438 F | $C_m$ | 39.5 F | $C_s$ | 103.4 F | | |
| $\tau_f$ | 1.75 s | $\tau_m$ | 215 s | $\tau_s$ | 1477 s | | |

***Table 4 Scaled model parameters for a 6-cell ultra-capacitor string***

The maximum module current that can be stored or discharged from a given ultracapacitor is given as:

$$I = \frac{V_r C_0}{T}$$

where T=15 s in our investigations. The replicated module of 6 cells rated 2500F is therefore restricted to a maximum 400A pulse in order to not over voltage the module. The input current and module voltage for the module circuit of Figure 5 is shown in Figure 7 below along with its FRF to an input current ac sweep.

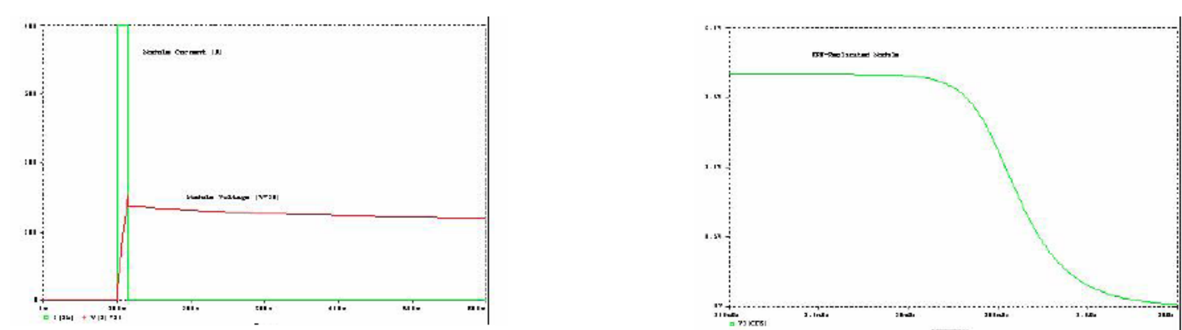

***Fig. 7 Replicated module time response to 400 A current pulse and frequency response***

**Maxwell Technologies, Inc.**
**Worldwide Headquarters**
9244 Balboa Avenue
San Diego, CA 92123
USA
Phone: +1 858 503 3300
Fax: +1 858 503 3301

**Maxwell Technologies SA**
CH-1728 Rossens
Switzerland
Phone: +41 (0)26 411 85 00
Fax: +41 (0)26 411 85 05

**Maxwell Technologies GmbH**
Brucker Strasse 21
D-82205 Gilching
Germany
Phone: +49 (0)8105 24 16 10
Fax: +49 (0)8105 24 16 19

**Maxwell Technologies, Inc. - Shanghai Representative Office**
Rm.2104, Suncome Liauw's Plaza
738 Shang Cheng Road
Pudong New Area
Shanghai 200120, P.R. China
Phone: +86 21 5836 5733
Fax: +86 21 5836 5620

**info@maxwell.com – www.maxwell.com**

The frequency response function for the replicated module of Figure 5 is performed by a frequency sweep over five decades. The resultant –3 dB point occurs at a frequency of 90 mHz. From this, the dominant time constant of the ultracapacitor module is found to be:

$$\tau = \frac{0.159}{f} = \frac{0.159}{0.090} = 1.77s$$

which agrees well with the data in Table 1 for the fast branch.

Next, the same simulation is performed, but for the scaled model representing 6 each, 2500F cells in series. The data listed in Table 4 is then used in a PSPICE net list. The results for an input 400A current pulse and FRF are shown in Figure 8.

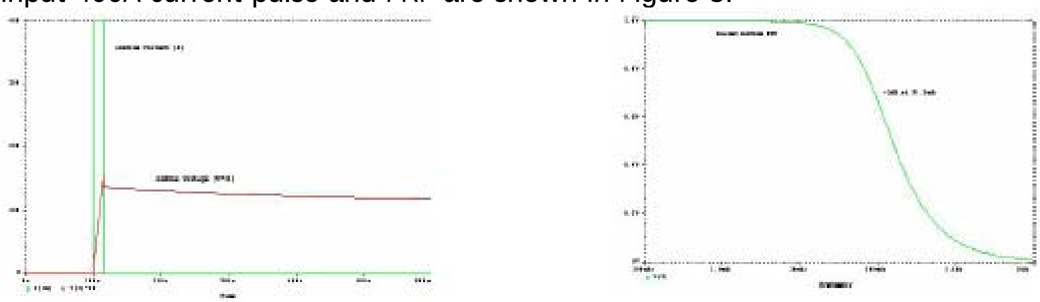

*Fig. 8 Ultra-capacitor data scaled to N=6 cell module*

The frequency response function for the scaled ultracapacitor model results in a dominant time constant of:

$$\tau = \frac{0.159}{f} = \frac{0.159}{0.0912} = 1.743s$$

which is good for the order of approximation employed in the scaling rules.
The short term ultracapacitor
model can also be viewed as a particular case of a Foster II electrical network consisting of R's and C's
that is also applicable for scaling considerations [8]. In its basic form, the admittance function for the Foster II network is:

**Maxwell Technologies, Inc.**
**Worldwide Headquarters**
9244 Balboa Avenue
San Diego, CA 92123
USA
Phone: +1 858 503 3300
Fax: +1 858 503 3301

**Maxwell Technologies SA**
CH-1728 Rossens
Switzerland
Phone: +41 (0)26 411 85 00
Fax: +41 (0)26 411 85 05

**Maxwell Technologies GmbH**
Brucker Strasse 21
D-82205 Gilching
Germany
Phone: +49 (0)8105 24 16 10
Fax: +49 (0)8105 24 16 19

**Maxwell Technologies, Inc. -**
**Shanghai Representative Office**
Rm.2104, Suncome Liauw's Plaza
738 Shang Cheng Road
Pudong New Area
Shanghai 200120, P.R. China
Phone: +86 21 5836 5733
Fax: +86 21 5836 5620

**info@maxwell.com – www.maxwell.com**

$$\frac{Y(s)}{s} = \frac{(s+\alpha_1)(s+\alpha_3)}{(s+\alpha_2)(s+\alpha_4)}$$

$$Y(s) = Hs + k_0 + \frac{k_2 s}{s+\alpha_2} + \frac{k_4 s}{s+\alpha_4}$$

where the partial fraction expansion of the admittance can be seen to approximate the short term model of the ultracapacitor given in Figure 4. The values of the individual coefficients are taken as the residues at the admittance poles; Y(s=0)=k0, Y(s=a2)= k2, etc. The parameter "a" is the reciprocal of each time constant. Figure 9 illustrates the Foster II circuit configuration. In Figure 10 the basic short term model given in Figure 4 is slightly modified to fit the Foster II equivalent and then transformed to its Cauer I equivalent.

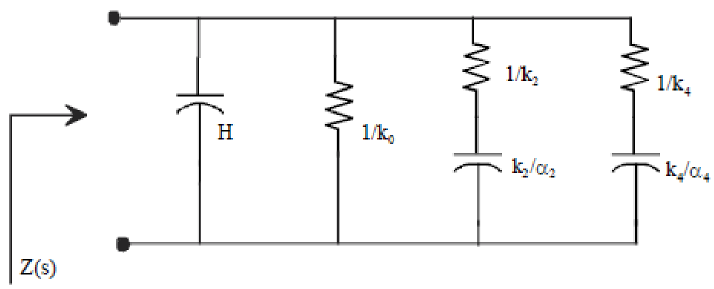


***Fig. 9 Foster II network approximation of an ultra-capacitor***

The Cauer I circuit representation gives somewhat more insight into the origins of the three time constant approximation of an ultracapacitor model. In this modified form the equivalent series resistance represents the combined effect of terminations, metal foil current collectors and its interfacial resistance to the carbon matte electrodes. The ESR term is separated from the short term model to facilitate the equivalent circuit transformation and included as ESR0. The resulting equivalent circuit then approximates the highly distributed nature of carbon matte resistance, ionic conduction, and Helmholtz double layer capacitances existing at macro, meso, and mircopores [9].

**Maxwell Technologies, Inc.**
**Worldwide Headquarters**
9244 Balboa Avenue
San Diego, CA 92123
USA
Phone: +1 858 503 3300
Fax: +1 858 503 3301

**Maxwell Technologies SA**
CH-1728 Rossens
Switzerland
Phone: +41 (0)26 411 85 00
Fax: +41 (0)26 411 85 05

**Maxwell Technologies GmbH**
Brucker Strasse 21
D-82205 Gilching
Germany
Phone: +49 (0)8105 24 16 10
Fax: +49 (0)8105 24 16 19

**Maxwell Technologies, Inc. - Shanghai Representative Office**
Rm.2104, Suncome Liauw's Plaza
738 Shang Cheng Road
Pudong New Area
Shanghai 200120, P.R. China
Phone: +86 21 5836 5733
Fax: +86 21 5836 5620

**info@maxwell.com – www.maxwell.com**

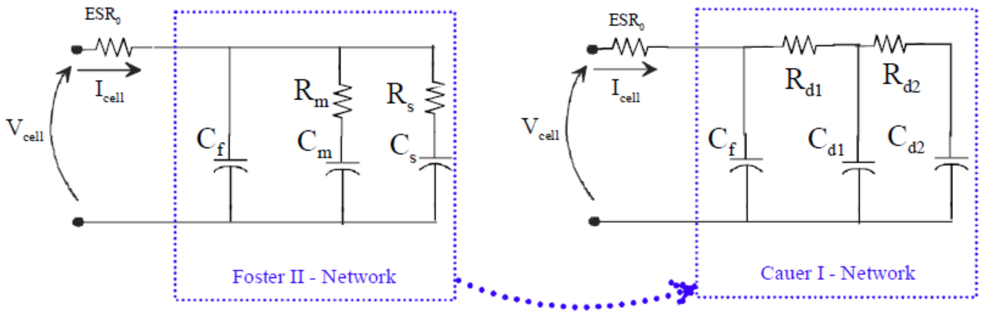


***Fig. 10 Network equivalents of ultra-capacitor short term model***

In Figure 10 the Foster II model parameters are carried over from Table 1 and transformed to the Cauer I equivalent by expanding the admittance function of the Foster II network by continued fractions. The admittance function of the Foster II network in Figure 10 is derived below. The resultant component values are listed in Table 5.

| Fast | | | | Medium | | | | Slow | | | |
|---|---|---|---|---|---|---|---|---|---|---|---|
| Foster II | | Cauer I | | Foster II | | Cauer I | | Foster II | | Cauer I | |
| $ESR_0$ | 0.68 mΩ | $ESR_0$ | 0.68 mΩ | $R_m$ | 0.8 Ω | $R_{d1}$ | 0.6268 Ω | $R_s$ | 2.9 Ω | $R_{d2}$ | 3.729 Ω |
| $C_f$ | 2600 F | $C_f$ | 2600 F | $C_m$ | 250 F | $C_{d1}$ | 246.75 F | $C_s$ | 560 F | $C_{d2}$ | 563 F |

***Table 5 Component values of Foster II and Cauer I equivalent circuit representations of ultra-capacitor cell***

$$Y(s) = \frac{C_f s^3 + [(\alpha_m + \alpha_s)C_f + 1/R_m + 1/R_s]s^2 + (\alpha_m \alpha_s C_f + \alpha_s/R_m + \alpha_m/R_s)s}{s^2 + (\alpha_m + \alpha_s)s + \alpha_m \alpha_s}$$

$$Y(s) = \frac{2600s^3 + 16.197s^2 + 1.0502x10^{-2}s}{s^2 + 5.616x10^{-3}s + 3.08x10^{-6}}$$

$$Y(s) = 2600s + \cfrac{1}{0.6268 + \cfrac{1}{246.75s + \cfrac{1}{3.729 + \cfrac{1}{563s}}}}$$

It can be seen by inspection of Table 5 that either representation of the ultracapacitor results in component values that are very similar, but where the Cauer I representation may be more appealing because of its correspondence to the physical structure of the electrodes. Either of these alternative representations may be used in the generic scaling approach discussed earlier.

**Maxwell Technologies, Inc.**
**Worldwide Headquarters**
9244 Balboa Avenue
San Diego, CA 92123
USA
Phone: +1 858 503 3300
Fax: +1 858 503 3301

**Maxwell Technologies SA**
CH-1728 Rossens
Switzerland
Phone: +41 (0)26 411 85 00
Fax: +41 (0)26 411 85 05

**Maxwell Technologies GmbH**
Brucker Strasse 21
D-82205 Gilching
Germany
Phone: +49 (0)8105 24 16 10
Fax: +49 (0)8105 24 16 19

**Maxwell Technologies, Inc. -**
**Shanghai Representative Office**
Rm.2104, Suncome Liauw's Plaza
738 Shang Cheng Road
Pudong New Area
Shanghai 200120, P.R. China
Phone: +86 21 5836 5733
Fax: +86 21 5836 5620

**info@maxwell.com – www.maxwell.com**

## 3. Multiple Zone Energy Buffering

Vehicle electrical systems have evolved to multiple zones in terms of not only power distribution, but communications networks as well. Luxury class vehicles may have three or more load centers dispersed in vehicle package zones according to the option content. The basic zones in for example the Jaguar XK, are located in the under hood, instrument panel, and trunk areas. Each of these zones is fed by individual power mains to local power distribution panels containing fuses and circuit breakers for the various modules. In addition, there may be Class A and Class B multiplex for low and medium speed functions and higher speed networks such as audio system protocol, CAN, or other communications bus standard for infotainment systems. X-by-wire functionality for steering, braking, throttle and other essential vehicle functions are gaining popularity.

Cohen and Smith [10] introduced the concept of distributed power modules in the vehicles electrical system architecture. Distributed power modules located at critical loads such as near the electric power assist steering system module, or near electro-hydraulic brake modules offers the vehicle designer additional redundancy for such safety critical applications as well as the means to stiffen battery power at each remote location thus enhancing the performance of these systems. Electric assist steering is a prime example of a system that benefits from a distributed energy storage module to buffer fluctuations in battery voltage at the remote load. When the vehicle electrical system becomes overloaded due to heavy usage the voltage at the battery will sag and consequently some remote loads may suffer performance, particularly if these systems rely on dc brushed motors. A dc brush motor characteristic is very voltage sensitive and performance deteriorates when terminal voltage is reduced. The availability of a low impedance energy buffer in the vicinity of such motors helps sustain their function over the anticipated usage cycle. A derivation of the necessary module ratings for various systems applications and for specified module power requirements are described in [11]. In that work a methodology is given that relates functional power demand and usage time to ultracapacitor size and current rating.

Figure 11 illustrates the major vehicle functions that are of interest for distributed energy buffers. The lowest level of the systems architecture contains the sensors and actuators needed by each function. For example, power assist steering requires input from the steering wheel for angle and torque in order to deliver the proper assist to the steering rack regardless of road condition, cross wind, or handling maneuvers. Similar requirements apply for braking and engine throttle control.

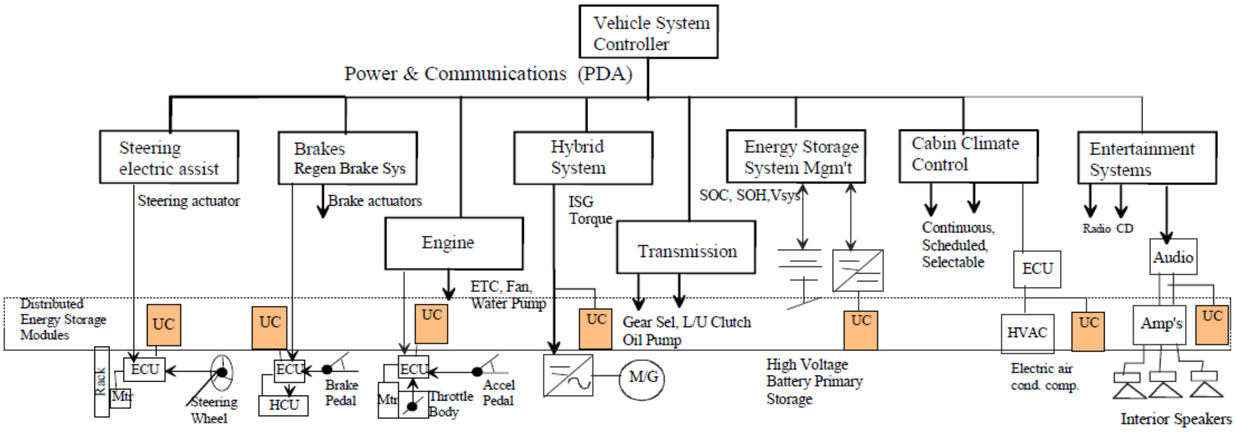


*Fig. 11 Vehicle electrical system hierarchy and zonal locations*

The merits of ultracapacitor energy buffers can be illustrated by taking four specific functions from the various package zones illustrated in Figure 11. Electric steering and brakes are located in the chassis zone, the hybrid system is located on the power train, typically in the under hood zone, and the audio and entertainment system is generally located in the trunk package tray zone. The peak power and usage of these functions are summarized in Table 6 along with calculations of their respective current requirements and energy buffer capacity, current, time constant assuming >85% discharge efficiency, and module ESR and capacitance.

| Load | Load Power, P | Usage Time, T | Stored Energy, $W_0$ | Rated Current, $I_r$ | Module Capacity, $C_m$ @ $\tau$>85% | Module Current, $I_c$, | Module Time Constant, $\tau$, | Module ESR | Cell Cap. $C_{cell}$ |
|---|---|---|---|---|---|---|---|---|---|
| (units) | kW | s | kJ | A @ V | F | A | s | mΩ | F |
| Electric Steer | 1.2 | 3 | 3.6 | 28.6@ 42V | 6.4 | 45 | 0.23 | 35 | 128 |
| Electric brake | 2 | 3 | 6 | 47.6@ 42V | 10.7 | 75 | 0.23 | 21 | 214 |
| Hybrid M/G | 50 | 15 | 750 | 139@ 360V | 18.2 | 218 | 1.125 | 62 | 2615 |
| Audio Amp. | 1.5 | 1.5 | 2.25 | 107@ 14V | 36 | 168 | 0.1125 | 3.12 | 216 |

*Table 6 Distributed energy buffer requirements in a multiple zone electrical system*

where derivation of module sizing for capacitance and current are given in [11]. The module time constant is derived from the relationship between ultracapacitor discharge efficiency, hd, and time interval, T, for full depletion:

$$\eta_d = 1 - 2\frac{\tau}{T} >= 0.85$$

and where module capacitance is derived from the working voltage as specified (and from which the required cell count is obtained). The module ESR is then calculated from the required module time constant needed to insure the specified discharge efficiency.

The hybrid M/G requirement is particularly interesting. The time interval of discharge was fixed at 15s so that the ultracapacitor is sufficient to maintain propulsion power over the entire 060 mph acceleration interval of the vehicle. The needed energy corresponds to some 208 Wh being discharged at 218 A and 360V into the traction inverter in the example given by Figure 2. A dc/dc converter booster is present in the electric drive line to maintain the dc bus voltage. For example, if the vehicle is a fuel cell hybrid with a 3.3 kW/s response the ultracapacitor boosting power will have the profile shown in Figure 12.

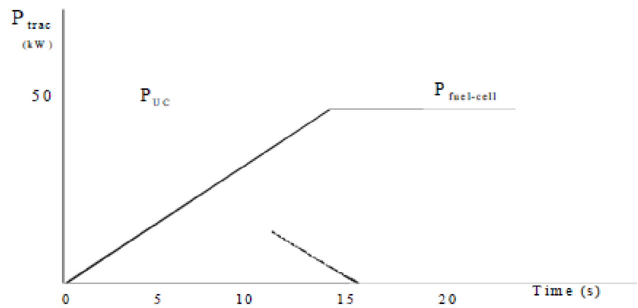


*Fig. 12 Fuel cell hybrid with ultra-capacitor buffer*

Other applications of energy buffers can be envisioned for LED tail lighting, high intensity discharge (HID) headlights, and other lighting options. Electric active suspension is a particularly attractive application of ultracapacitors due to its short term, high burst power, actuator requirements. During normal road driving the active suspension system on a midsized vehicle will draw approximately 120W of average power, but its instantaneous power at each wheel strut may reach +/6 kW. Local energy buffers at each corner unit would provide the necessary level of battery reinforcement in this highly distributed electrical system load. A further illustration of ultracapacitor energy buffering applied to a grid connected hybrid vehicle is considered in the next section.

## 4. Ultracapacitor Energy Buffering in a Grid Connected Hybrid

A recent EPRI study [12] defined four base case vehicle configurations:

1. A conventional vehicle (CV) with an internal combustion engine that serves as an overall baseline for the comparison of vehicle attributes.

2. A parallel hybrid with a small battery for power assist and regenerative braking but no plug-in capability and no all-electric range (HEV0). This type of vehicle is the current conception of a “hybrid” vehicle by the U.S. automotive industry.
3. A parallel hybrid that can operate like an HEV0 but also has grid plug-in recharge capability and a battery of sufficient capacity to provide at least 20 miles of all-electric range (HEV20).
4. A parallel hybrid similar to the HEV20 but with a battery of sufficient capacity to provide at least 60 miles of all-electric range (HEV60).

These base case vehicles are loosely based on the 2000 model year Chevrolet Lumina midsize vehicle and are intended to have similar automotive performance, acceleration, top speed, payload, etc. The vehicles differ principally in the details of their respective drive train configurations and in the amount of onboard electric energy storage. A follow on study, in which one of the authors participated, further considered the HEV20 vehicle and sought to determine whether or not the addition of ultracapacitor energy storage would improve the overall economic and automotive performance of the vehicle. The modified HEV20 vehicle was designated as the HEV20U, the U standing for the addition of ultracapacitors.

In a vehicle, range requires energy and performance requires power. In the original HEV20 vehicle a NiMH battery pack provided both the energy, 5.9 kW hr, needed to travel 20 miles in the all-electric mode of operation and the instantaneous power, 54 kW, needed to provide adequate vehicle automotive performance, principally acceleration. In the HEV20U vehicle a battery pack would also supply the 5.9 kW hr energy requirements but the ultracapacitor pack would supply the major portion of the vehicle’s peak power needs. The design of the HEV20U vehicle would then center on the tradeoffs between the type, size, and ratings of the battery and ultracapacitor storage devices. To quantify these tradeoffs several HEV20U configurations with different, currently available ultracapacitor packs were compared via calculation of their performance over a common, fixed drive cycle. Automotive performance was calculated using the public domain Matlab/Simulink program Advisor, written and maintained by DOE’s National Renewable Energy Laboratory (NREL) in Golden, CO; and the common vehicle drive cycle used for comparison was the Federal Urban Driving Schedule (FUDS). The FUDS cycle is well known, accepted as realistic, and is representative of the type of city driving for which a hybrid vehicle, with an all-electric mode capability, should (hopefully) be able to demonstrate an economic and environmental advantage over its CV or HEV0 counterpart.

Here we present the results of only one case considered in the EPRI follow on study: all electric driven propulsion of the HEV20U vehicle over the FUDS cycle. The instantaneous electric power required of the HEV20U vehicle Electric Storage System (ESS) over the 1370 second drive cycle,

**Maxwell Technologies, Inc.**
**Worldwide Headquarters**
9244 Balboa Avenue
San Diego, CA 92123
USA
Phone: +1 858 503 3300
Fax: +1 858 503 3301

**Maxwell Technologies SA**
CH-1728 Rossens
Switzerland
Phone: +41 (0)26 411 85 00
Fax: +41 (0)26 411 85 05

**Maxwell Technologies GmbH**
Brucker Strasse 21
D-82205 Gilching
Germany
Phone: +49 (0)8105 24 16 10
Fax: +49 (0)8105 24 16 19

**Maxwell Technologies, Inc. - Shanghai Representative Office**
Rm.2104, Suncome Liauw’s Plaza
738 Shang Cheng Road
Pudong New Area
Shanghai 200120, P.R. China
Phone: +86 21 5836 5733
Fax: +86 21 5836 5620

**info@maxwell.com – www.maxwell.com**

as determined by the Advisor program, is given in Figure 13, and the resultant energy draw is given in Figure 14. The peak demand electric power is seen to be approximately 40 kW and the total energy required to complete the cycle is approximately 1.7 kWhr (note there is an assumed constant 500 W accessory load included in addition to the vehicle dynamic automotive load). The existing HEV20U battery pack and its attendant power electronic dc/dc converter is designed to deliver a constant, "average" power of 4400 Watts (1.7 kWhr averaged over 1370 seconds) to the traction inverter. The ultracapacitor pack then must make up the difference between the constant battery power and the demand power as given in Figure 13.

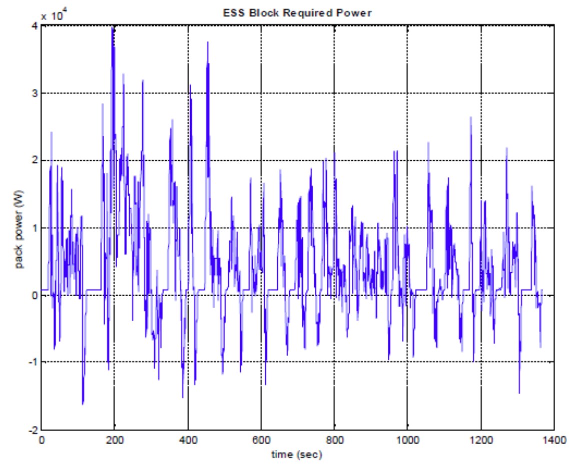


*Fig. 13 HEV20U Instantaneous Power Demands over FUD's Drive Cycle (Wx10$^4$)*

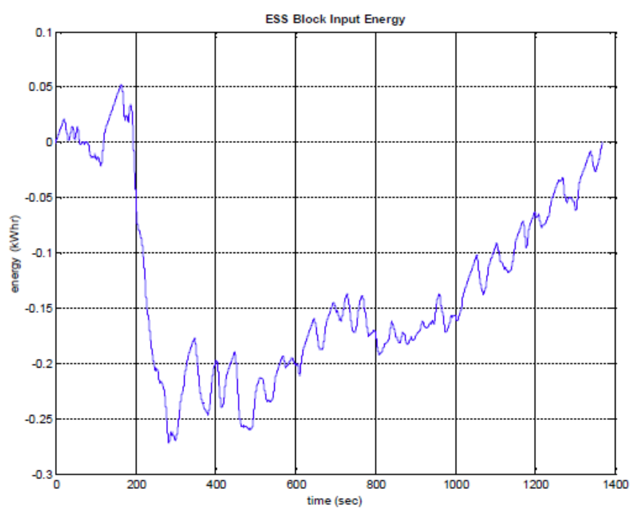


*Fig. 14 HEV20U Energy Demand over FUD's Drive Cycle (kWh)*

Calculated results for an ultracapacitor pack made up of 230 series connected Maxwell TC2700 cells (138 kg total cell mass) are given in Figure 15. The pack stored energy is seen to fall to approximately 0.3 kWhr due to a prolonged (100 second) period of power draw averaging approximately 10 kW starting at 200 seconds into the cycle. The pack stored energy then remains fairly constant until it recovers during the last 400 seconds of the cycle. This pattern, limited fall and eventual recovery, is also seen in the pack State of Charge and normalized terminal voltage.

Similar results have been calculated for other ultracapacitor pack configurations using cells from other manufactures. The overall results of the EPRI study indicate that the addition of ultracapacitors to a hybrid vehicle electrical energy storage system significantly lowers the peak power requirement of the battery pack. In the base case HEV20U vehicle, with simple constant battery power control, the required battery power rating was shown to be lowered by a factor of nine. Different battery technologies can thus be considered for a hybrid vehicle. In a battery only hybrid vehicle the dual power/energy requirements restrict the choice of usable battery technologies to the newer and more costly NiMH and Lithium based cells. But in a battery/ultracapacitor vehicle the choice of battery types is far more open. Previously discarded, for reasons of lower power density, but potentially lower cost, battery chemistries such as Feair, can now be reconsidered.

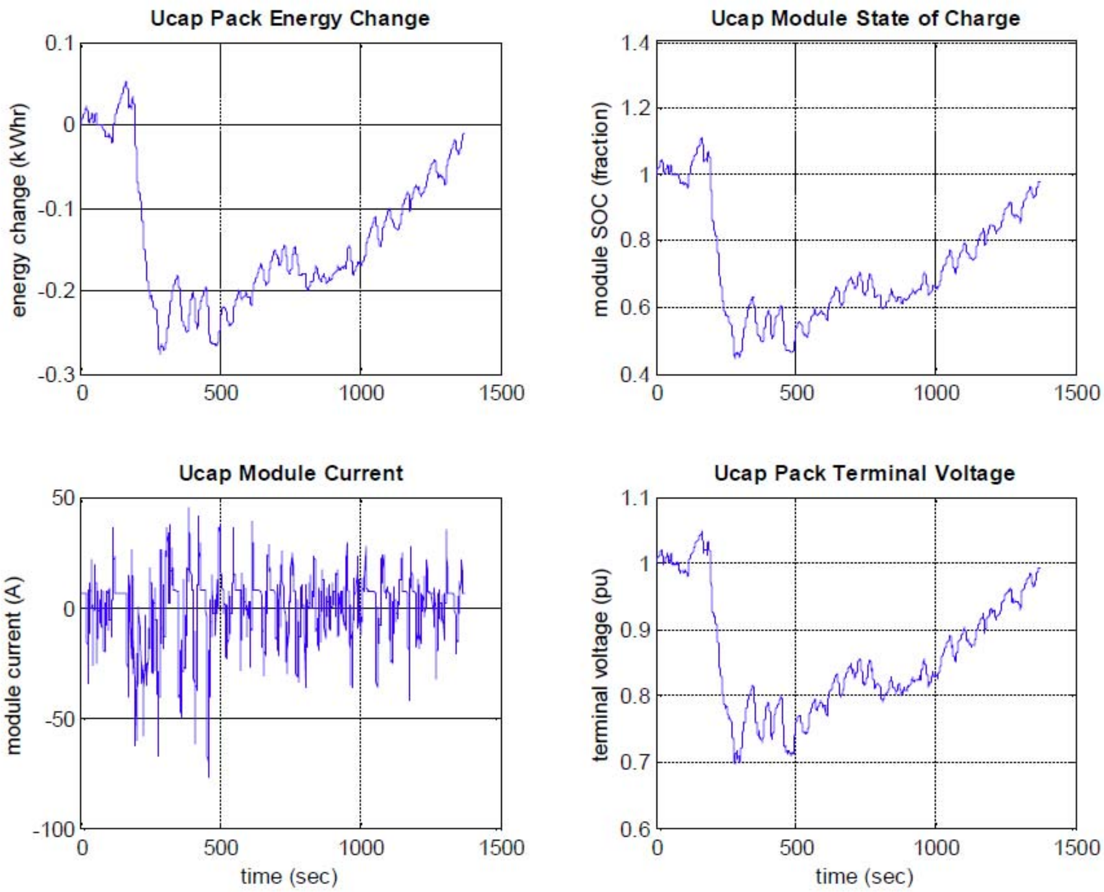


*Fig. 15 HEV Ultra-capacitor Energy Storage Pack for 20 Mile Electric Only Range (575V, 138 kg)*

## 5. After Market Applications

Today the audio after market application of high power amplifiers for low end boosting of the audio spectrum have turned to the use of ultracapacitors as the means of battery reinforcement. High values of capacitance in the past have been provided by large aluminum electrolytic capacitors located within 18 inches of the power amplifiers. Recently, carbon capacitors [13,14] are being applied due to their ability to source high currents for several seconds thus maintaining the amplifier power supply voltage with minimal droop compared to the use of aluminum electrolytic capacitors. Table 7 illustrates the comparison between typical after market audio system reinforcement capacitors that are generally mounted at the amplifier terminals and packaged in the vehicles trunk.

| | Capacitor Rating/Part No. | | Surge Voltage, (V) | Tolerance (%) | Pkg. Vol., (liters) | ESR, (mΩ) | Rated current, (A) | Peak current, (A) |
|---|---|---|---|---|---|---|---|---|
| Aluminum Electrolytic | 0.5 F | CPC05-03 | 20 | -10, +50 | 0.75 | <0.002 | | |
| | 1.0 F | CPC10-03 | 20 | -10, +50 | 1.0 | <0.002 | | |
| Carbon-cap (ultra-cap) | 25 | CPCC25 | 17.1 | -10, +30 | 3.9 | <14 | 40 | 250 |
| | 40 | CPCC40 | 17.1 | -10, +30 | 3.9 | <8 | 65 | 400 |

***Table 7 Audio system reinforcement capacitor comparison of technologies***

After market audio system woofers are generally rated 500 W average, and 1500 W peak. Heavy gauge wiring with appropriately rated circuit protection are installed beneath the cabin carpeting to distribute battery power to the audio amplifiers as shown in Figure 16. Fuses are installed within 18” of the battery terminal and at the load center power distribution block that is added in the vehicle trunk. At a nominal 13.5 Vdc the reinforcement capacitor will supply peaks of 112 A. Without the added voltage stiffening afforded by the reinforcement capacitor the amplifier voltage would droop significantly and degrade the audio quality. Low voltage carbon capacitors are unable to match the aluminum electrolytic ESR, but do provide far more energy buffering than available electrolytics. The last row in Table 6 is representative of the reinforcement capacitor specifications based on application requirements.

Inspecting the layout and installation of such high power audio system boosters it is apparent that a 42V vehicle electrical system would be far more desirable than adding all the weight and bulk associated with a 14 V system. Ultracapacitor modules rated at 42V are now available that would provide superior energy buffering.

**Maxwell Technologies, Inc.**
**Worldwide Headquarters**
9244 Balboa Avenue
San Diego, CA 92123
USA
Phone: +1 858 503 3300
Fax: +1 858 503 3301

**Maxwell Technologies SA**
CH-1728 Rossens
Switzerland
Phone: +41 (0)26 411 85 00
Fax: +41 (0)26 411 85 05

**Maxwell Technologies GmbH**
Brucker Strasse 21
D-82205 Gilching
Germany
Phone: +49 (0)8105 24 16 10
Fax: +49 (0)8105 24 16 19

**Maxwell Technologies, Inc. - Shanghai Representative Office**
Rm.2104, Suncome Liauw's Plaza
738 Shang Cheng Road
Pudong New Area
Shanghai 200120, P.R. China
Phone: +86 21 5836 5733
Fax: +86 21 5836 5620

**info@maxwell.com – www.maxwell.com**

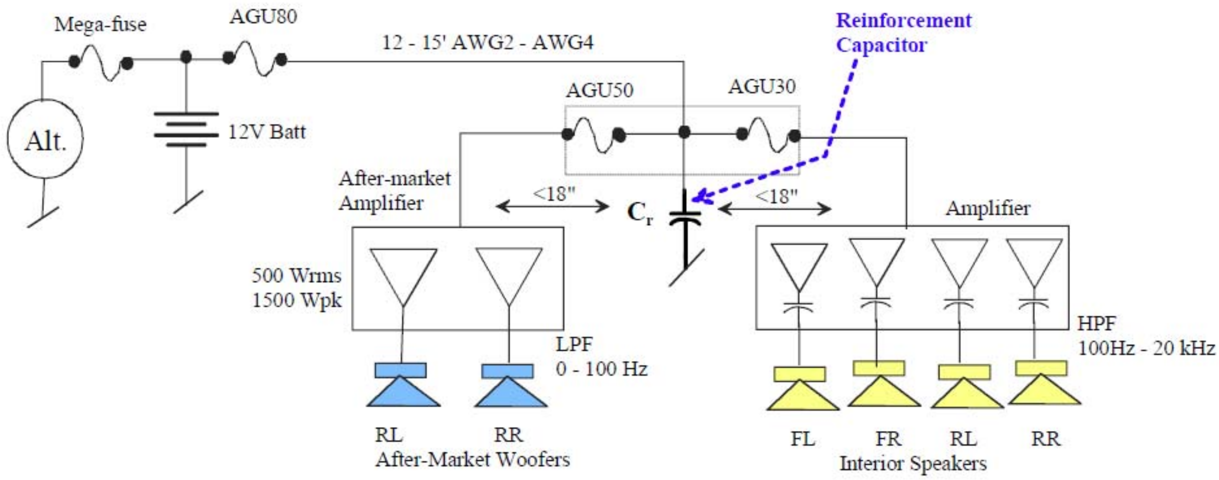


*Fig. 16 Audio system after market installation*

Other after market applications for ultracapacitors are as local energy buffers for pickup truck snow plow equipment. This equipment is very popular in Northern states but has not included ultracapacitor buffering. The added equipment consists of a battery relay and 2 AWG cable to connect 14V power a 2.5 kW or higher rated electric motor driven hydraulic pump. Peak power is 5.5 kW or higher under load. Load current is typically 300A to 700A depending on blade loading and with durations of fractions of a second to 1.5 seconds. The high power, intermittent usage is very demanding of the battery and results in early wear out, primarily through cycling at cold temperatures and low charge rates. Figure 17 is representative of snowplow actuation inrush and load current as the blade is lifted under load against a snow bank.

**Maxwell Technologies, Inc.**
**Worldwide Headquarters**
9244 Balboa Avenue
San Diego, CA 92123
USA
Phone: +1 858 503 3300
Fax: +1 858 503 3301

**Maxwell Technologies SA**
CH-1728 Rossens
Switzerland
Phone: +41 (0)26 411 85 00
Fax: +41 (0)26 411 85 05

**Maxwell Technologies GmbH**
Brucker Strasse 21
D-82205 Gilching
Germany
Phone: +49 (0)8105 24 16 10
Fax: +49 (0)8105 24 16 19

**Maxwell Technologies, Inc. - Shanghai Representative Office**
Rm.2104, Suncome Liauw's Plaza
738 Shang Cheng Road
Pudong New Area
Shanghai 200120, P.R. China
Phone: +86 21 5836 5733
Fax: +86 21 5836 5620

**info@maxwell.com – www.maxwell.com**

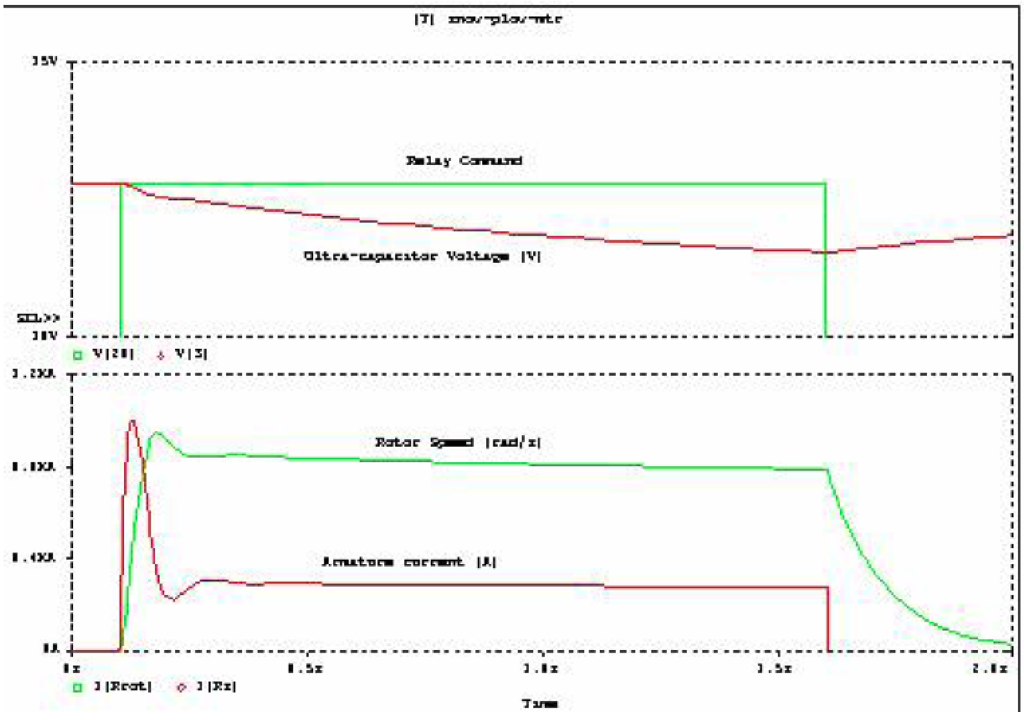


*Fig. 17 Electro-hydraulic snow plow after market application for ultra-capacitors*

For this application an ultracapacitor module rated 214 F at 16V (17.1 V surge) with a peak discharge current of 784 A at a discharge efficiency of 85%. The ultracapacitor terminal voltage droops by 1 volt under load when the pump current is 300A. This size ultracapacitor would be sufficient to provide the needed energy buffering and minimize wear out of the vehicles battery.

## 6. Conclusions

This paper has presented several applications of how distributed energy buffers would enhance system functionality as battery surrogates. High power, highly intermittent loads having peak to average power demands exceeding 6:1 are best serviced by local energy buffers sized to each particular function. Hybrid and fuel cell vehicles are already being designed with ultracapacitor Boosters to augment conventional batteries, engine driven generators, and fuel cell power plants during transient conditions. Grid connected hybrids are another niche application where high pulse power is required. Emerging X-by-wire functionality will demand either more distributed battery systems in the vehicle for safety critical functions, or more widespread application of ultracapacitor energy buffers to meet the demands for stiff vehicle power supply. Today's after market applications already are taking advantage of ultracapacitors to bolster audio system performance when the high power amplifiers are located far from the vehicles battery. Use of two, three of more electrochemical batteries for such functions is one approach, but the necessity for long service life, low maintenance especially when such distributed battery systems are packaged in remote locations will be problematic. Ultracapacitors are more suitable energy buffers since they provide flexible sizing to suit vehicle segment and functional needs, are capable of operation of wide temperature extremes without degraded performance, and offer cycle life sufficient to meet durability of 6 to 10 years at >100,000 deep cycles.

## References


1. Automotive Engineering International, global vehicles pgs 1416, Dec. 2002
2. See, US Fuel Cell Council at www.usfcc.com
3. K. Miyadera, "Development of ES 3 Small Sized LowFuel Consumption Vehicle," Toyota Technical Review, Vol. 52, No. 1, Sept. 2002, pgs. 2227
4. P. Rodatz, O. Garcia, L. Guzzella, F. Buchi, G. Scherer, A. Wokaun, "Performance and Operational Characteristics of a Hybrid Vehicle Powered by Fuel Cells and SuperCapacitors," SAE International publication 2003010418, SAE special publication SP1741, Fuel Cell Power for Transportation 2003.
5. I. Hwang, SH. Kim, NH. Kim, JH. Lee, SH. Choi, YS. Yoon, "Development of Fuel Cell Hybrid Electric Vehicle Fueled by Methanol," ibid
6. A. Di Napoli, F. Crescimbini, L. Solero, F. Caricchi, F. G. Capponi, "MultipleInput DcDc Power Converter for Power Flow Management in Hybrid Vehicles," IEEE Industry Applications Society Annual Meeting, Omni William Penn Hotel, Pittsburg, PA. Oct. 1317, 2002
7. D. New, J. G. Kassakian, J. Schindall, "Automotive Applications of Ultracapacitors," MIT/Industry Consortium on Advanced Automotive Electrical/Electronic Components and Systems, Consortium Project Report Winter 2003
8. Adam Budak, Passive and Active Network Analysis and Synthesis, Houghton Mifflin Company, Boston 1974
9. J. Schindall, J. Kassakian, D. Perreault, D. New, "Automotive Applications of Ultracapacitors: Characterizatics, Modeling and Utilization," MITIndustry Consortium on Advanced Automotive Electrical/Electronic Components and Systems, Spring Meeting, RitzCarlton Hotel, Dearborn, MI. March 56, 2003
10. M. Cohen, R. Smith, "Application of Distributed Power Modules on 42V Systems," Global Powertrain Conference, Advanced Propulsion Systems, Sheraton Inn Hotel, Ann Arbor, MI. Sept. 2426, 2002, pgs 76-79.
11. J.M.Miller, R. Smith, "Ultracapacitor Assisted Electric Drives for Transportation," International Electric Machines and Drives Conference, Hilton Monona Terrace Hotel, Madison, WI. June 14, 2003
12. EPRI Report TR1000349, "Comparing the Benefits and Impacts of Hybrid Electric Vehicle Options", July 2001
13. Installation and Application Manual, 0.5 Farad and 1.0 Farad Reinforcement Capacitor, www.rockfordfosgate.com
14. Installation and Application Manual, 25 Farad and 40 Farad Reinforcement Capacitor, www.rockfordfosgate.com